4.1 Introduction

The main diagnostics used in the present work were miniature magnetic probes, which were inserted into the re-entrant glass probe guides described in Section 3.2. Externally integrated conventional wire-wound probes were used to make detailed measurements of the magnetic field produced by the quasi-steady driven plasma currents. These probes were also used with limited success to study the penetration of the RF magnetic field into the plasma. Hall effect magnetic probes, as described by KIROLOUS(1986), with dimensions similar to the wire-wound probes were also used. The Hall probes were used primarily to calibrate the vertical field coils. A Hall probe was also used to determine the total amount of driven toroidal current. This was done by measuring the strength of the vertical magnetic field produced by the driven current at centre of the device. The toroidal current was continuously monitored with an externally integrated Rogowski belt wrapped around the minor section of the the discharge vessel. The Rogowski belt is described in Section 4.3.

4.2 Magnetic Field Probes

4.2.1 Wire-Wound Probes

An existing conventional wire-wound probe (Probe M4), with an overall length of 40cm, could be inserted into the minor section of the discharge vessel through the single probe guides shown in Figure 3.4. For detailed measurements using the probe guide array of Rythmac-1, a considerably longer and slightly smaller probe was required. Two identical magnetic probes each with a total length of 100cm were constructed for this purpose (Probes M5,M6). These probes were also used to perform detailed measurements on both later devices, Rythmac-2,3.

Each of the wire-wound probes (M4,M5,M6) were double probes which consisted of two coils mounted orthogonally so that two components of the time derivative of

the magnetic field could be measured simultaneously. One coil was orientated so as to measure the component of $\partial B/\partial t$ in the major radial (R) direction. The second coil was mounted so that it measured the vertical (Z) component of $\partial B/\partial t$. By rotating the magnetic probe about its axis through a quarter turn in either direction, the latter coil could be used to measure the toroidal (ϕ) component of $\partial B/\partial t$ rather than the vertical component.

The output voltage of each coil, V_o, is given by ;

$$V_o = -NA\frac{\partial B}{\partial t}$$

where, N, is the number of turns in the coil and, A, is the cross sectional area of each turn. The product, NA, is known as the effective area of the coil.

Each coil was wound from 50 turns of 46 SWG enamelled copper wire. The effective area of each coil was approximately $3cm^2$. The coil used to detect the major radial component of the magnetic field (when the output of the coil is externally integrated), consisted of a solenoidal coil of length 4mm and approximate diameter 3mm. The vertical or toroidal component of the magnetic field was detected with a rectangular coil of approximate dimensions $1.6 \times 4 \times 2$mm, consisting of two layers each of 25 turns. The b_Z coil was mounted inside the b_R coil. The coil structure was sealed in Araldyte epoxy resin for protection and mounted at the end of a 3mm OD stainless steel tube which was used to provide mechanical support and to shield the probe leads.

The magnetic probe voltage output signals were transmitted via triaxial cable to a Faraday cage which housed the signal electronics and data acquisition system. The probe leads were connected to the centre conductor and inner braid of the triax cable. The outer layer of the triax cable was connected to the stainless steel tube and was earthed at the Faraday cage so that it acted as an electrostatic shield for the probe signal.

Inside the Faraday cage the probe signals were processed as shown in Figure 4.1 and described here. The probe signal cables were terminated with their characteristic

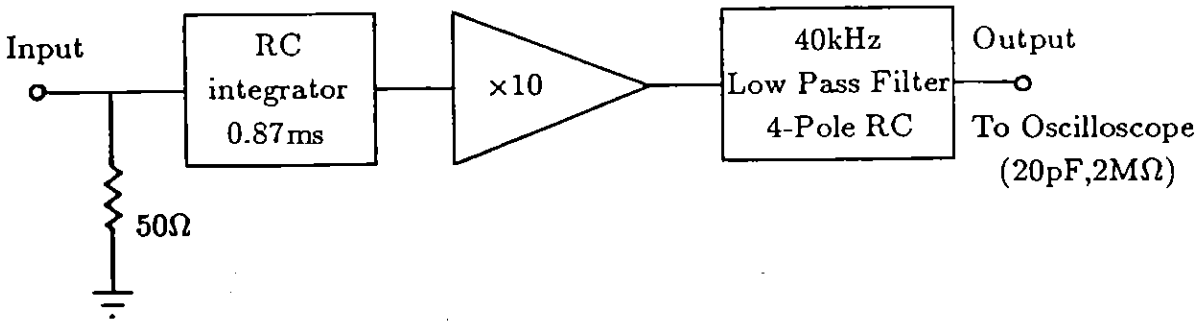

Figure 4.1 Signal Processing for the Wire-Wound Probes

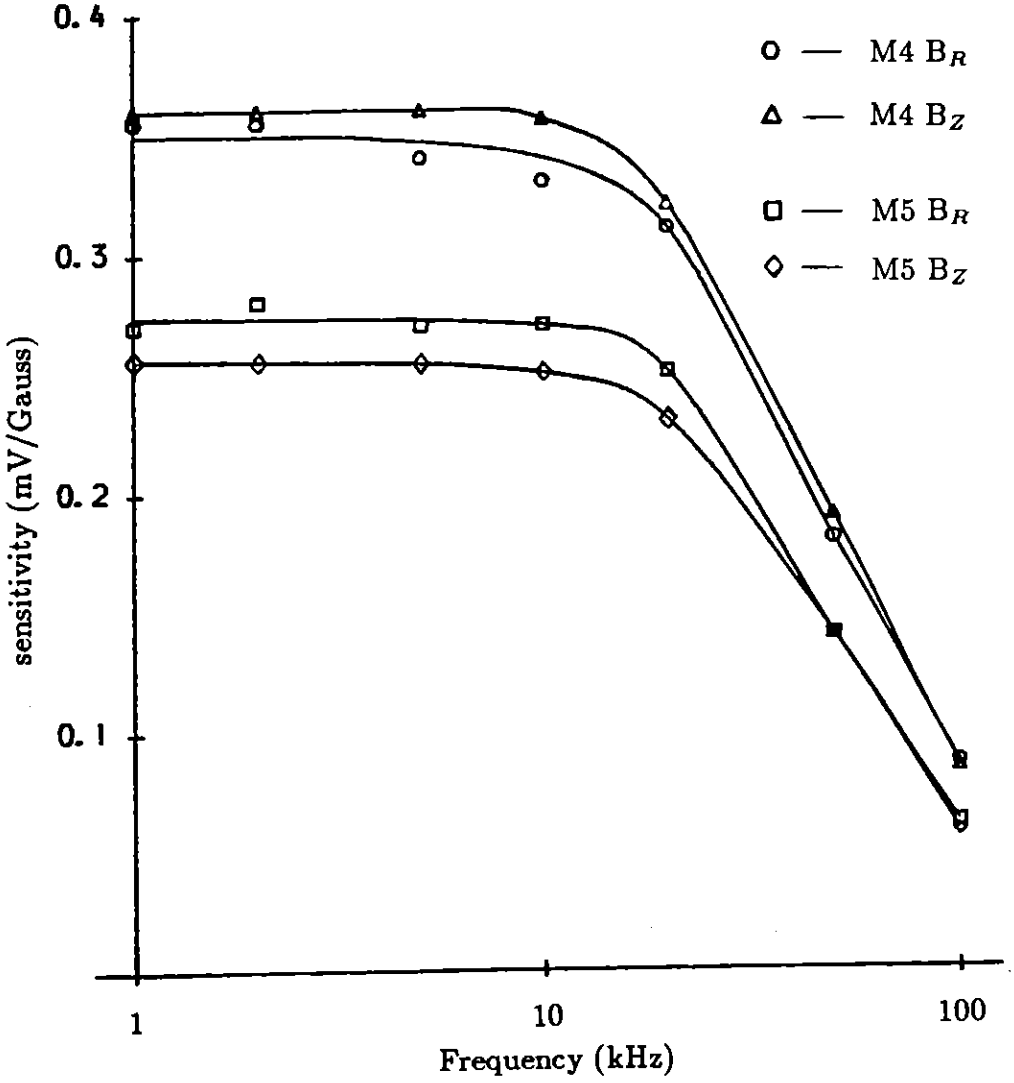

Figure 4.2 Frequency response of the Wire-Wound Probes M4,M5 for the arrangement shown in Figure 4.1. The responses of probes M5 and M6 are identical.

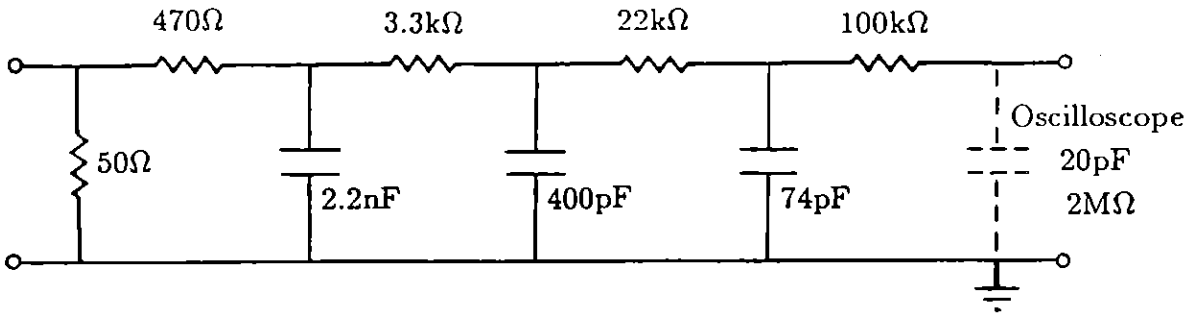

Figure 4.3 Circuit Diagram for the 4-Pole RC Low-Pass Filter.

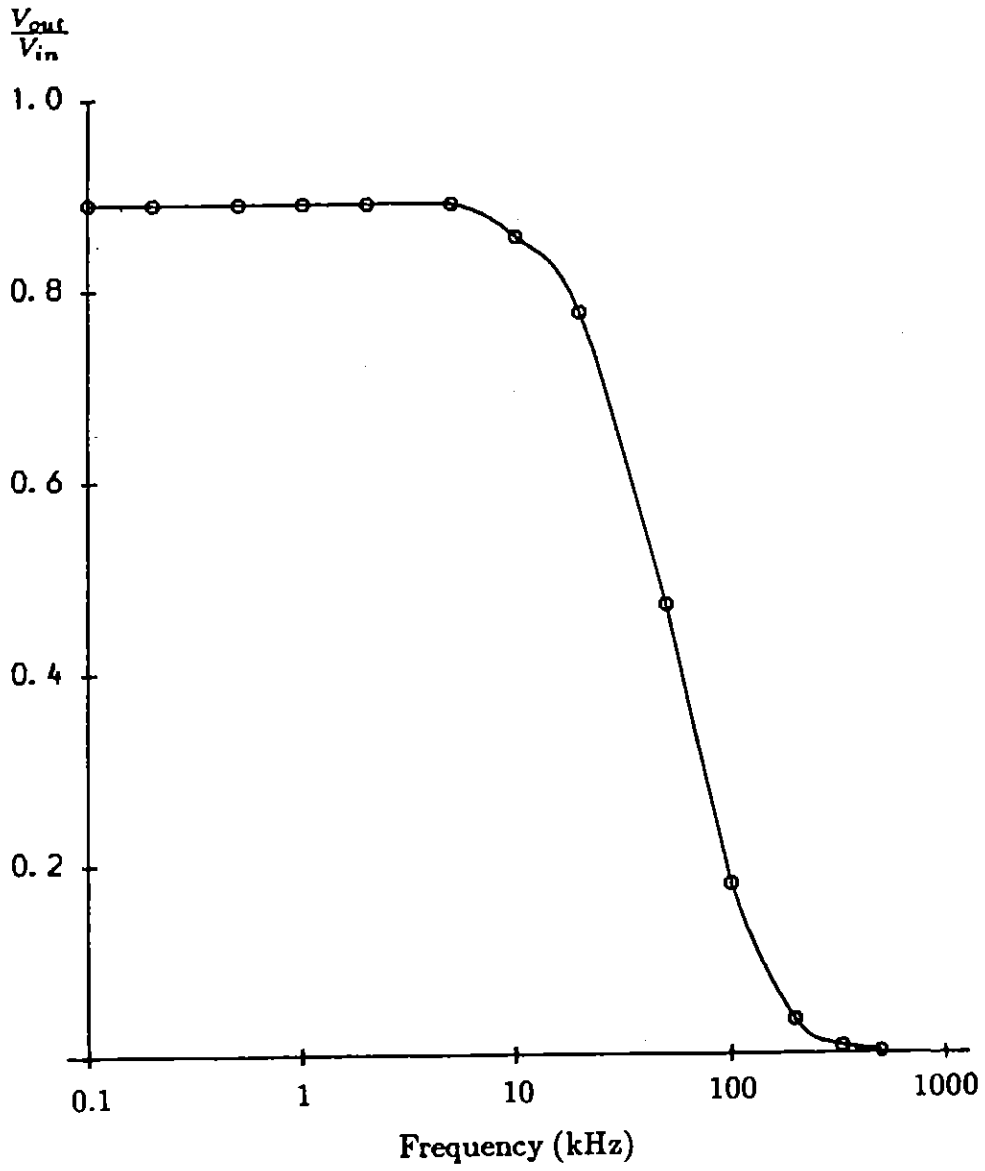

Figure 4.4 Frequency Response of the RC Low-Pass Filter shown in Figure 4.3.

impedance of 50Ω. The magnetic field of interest was recovered from the raw probe signal by integration using a passive integrator with a suitable RC time constant. An integrator with a time constant of 0.87ms was used to detect the magnetic field produced by the quasi-steady driven plasma current. In order to increase the probe signal size and improve the signal-to-noise ratio, the integrated probe signal was amplified (by a factor of 10) and then passively filtered, before being displayed on a Tektronics 468 digital storage oscilloscope. A 50Ω input impedance 4-pole RC low-pass filter with a sharp cutoff frequency (3dB point) of 40kHz was used to remove the large unwanted 330kHz RF components of the probe signal. The 20pF input capacitance of a Tektronics 468 oscilloscope formed part of the last filter stage. The measured insertion loss of the filter was −1.0dB. The circuit diagram for the lowpass filter is shown in Figure 4.3 and the measured frequency response of the filter is given in Figure 4.4.

The signal from the probe, including the effects of the integrator, amplifier and filter, was calibrated as a function of frequency using a sinusoidally varying magnetic field produced by a small (9.5cm diameter) Helmholtz coil. The current through the Helmholtz coil was supplied by a Perreaux 8000B power amplifier designed for audio frequencies, but which delivered a useful amount of power at frequencies up to 300kHz. The Perreaux amplifier was fed by a Datapulse 410 function generator. A calibrated Model 1025 Pearson current transformer (with a sensitivity of 0.025V/A) was used to monitor the Helmholtz coil current. The field at the centre of the Helmholtz coil was calculated and compared with the probe signal, which was displayed on an oscilloscope. In this way the probe sensitivity was obtained. Figure 4.2 shows the frequency dependence of the measured probe sensitivities for probes M4 and M5. The frequency response of probe M6 is identical to that of probe M5, to within the measurement error of several percent. The probe sensitivities at 20kHz were used in the analysis of the quasi-steady plasma magnetic field measurements. These sensitivities are listed in Table 4.1, together with the probe coil specifications.

probe	effective area (cm^2)	calibration (mV/Gauss)	DC Resistance (Ω)
M4 b_R	3.5	0.31	10
M4 b_Z	3.5	0.32	10
M5 b_R	3.0	0.25	16
M5 b_Z	2.8	0.23	16
M6 b_R	3.0	0.25	16
M6 b_Z	2.8	0.23	16

Table 4.1: Wire-Wound Magnetic Probe Specifications.

The roll-off of the lowpass filter (Figure 4.4) is seen to reduce the probe sensitivity at high frequencies. This reduction in probe sensitivity is expected to result in some loss of information concerning the high frequency (very short timescale) behaviour of the plasma. In order to overcome this problem, a much sharper filter would be needed to remove the very large RF component of the probe signal, which includes extraneous RF pickup. Alternatively, if more cycles of RF power could be made available, it would be more interesting to use magnetic probes to study the longer timescale behaviour of the plasma in preference to short term fluctuations or the "start-up" phase seen in the present experiments.

A wire-wound magnetic probe was used to examine the spatial dependence of the amplitude of the magnetic field produced by the quasi-steady driven plasma current and to extract the poloidal flux function, $\Psi_{pol} = \int ds \cdot B_{pol}$. This was done by recording the time history of the components of the magnetic field at a large number of locations on a rectangular grid in the minor section of the device. The positions of the probe in the grid were accurately relocatable using an array of probe guides. Cross-plotting was used to obtain data corresponding to the same time. Experimental measurements were made of the magnetic field components in the major radial and

vertical directions, (B_R,B_Z). The magnetic field data B_R(R,Z) and B_Z(R,Z) obtained by cross-plotting was numerically analysed using the method described in Chapter 5 to determine the poloidal flux to within an additive constant.

A magnetic probe was positioned in a selected probe guide and moved radially in or out of the minor section by means of an electronically controlled stepping motor and its associated drive mechanism. All probe guides were retracted to the outer wall when not in use. Only one probe guide in each of the probe guide arrays could be used at any given time. 'Droop' and minor non-uniformities in the probe guides prevented the magnetic probes from being located to better than 0.1cm.

4.2.2 Hall Effect Magnetic Probes

The steady magnetic fields of the Rythmac devices were measured with a magnetic probe based on a Hall effect element (Siemens type SBV 566 Hall Generator). The probe was similar in design and construction to that described by KIROLOUS(1986).

The design difference lay in the electronics used to supply the control current ($\sim$ 35mA) for the probe element as shown in Figure 4.5. The voltage across the element was regulated, rather than the current through the element. In hindsight, it would have been more satisfactory to regulate the control current by increasing the supply voltage and including a large fixed resistor in series with the Hall element, but this was not done. In the present design, the control current will be constant provided that the resistance of the Hall element does not change. The resistance of the element is not expected to vary greatly from the equilibrium value reached after the probe has been switched on for a few minutes. The element is also not expected to be heated significantly during experiments since the duration of each plasma shot is very short and the duty cycle for plasma shots is very low.

In the work presented here, the Hall probes were used primarily to calibrate the vertical magnetic field coils as described in Section 3.5. Here, the exact Hall probe sensitivity was unimportant, as the probe was used to compare the vertical magnetic

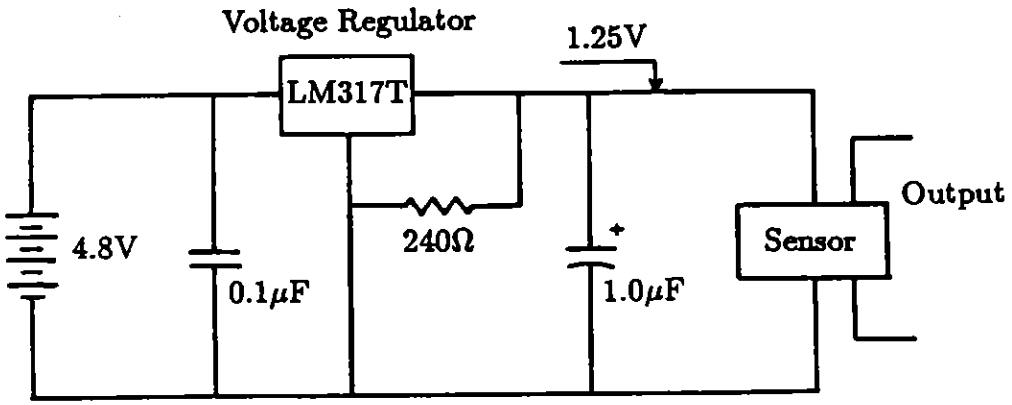

Figure 4.5 Circuit diagram for the voltage regulator used to generate the control current for a Hall effect magnetic probe.

field produced by the slow capacitor bank with the field produced when a known DC current was passed through the vertical field coils. A calibrated Hall probe was also used to determine the amount of driven toroidal current as mentioned in the following section.

4.3 Plasma Current Measurements

The amount of quasi-steady driven toroidal current can be easily determined with some degree of accuracy from a knowledge of the device geometry and a measurement of the vertical magnetic field produced by the current at the major axis of the machine. Such a measurement can be performed with a calibrated Hall probe. A more accurate determination of the total driven toroidal current using this method requires a detailed knowledge of the toroidal current density distribution in the minor section.

An externally integrated Rogowski Belt wrapped around the minor section of the device was used to provide a more reliable measurement of the driven toroidal current. The Rogowski belt was wound on the outside of the vacuum vessel, over the top of the RF windings. A separate Rogowski belt was constructed for each of the three Rythmac devices.

Each Rogowski coil consisted of a close wound solenoid of 1.0mm diameter enamelled copper wire, wound on a former of 15mm OD PVC tubing. A BNC coaxial connector was fastened to one end of the solenoid. The far end of the solenoidal coil returned back through its centre, inside the PVC tubing to the BNC connector. The Rogowski coil specifications are given in Table 4.2.

The Rogowski belt was wrapped around the minor section of the vacuum vessel and secured in place with string. The output of the Rogowski coil was transmitted via coaxial cable into the Faraday cage, where it was passively integrated and displayed on a Tektronics 468 digital storage oscilloscope. The RC time constant of each Rogowski coil integrator was very close to 0.85ms.

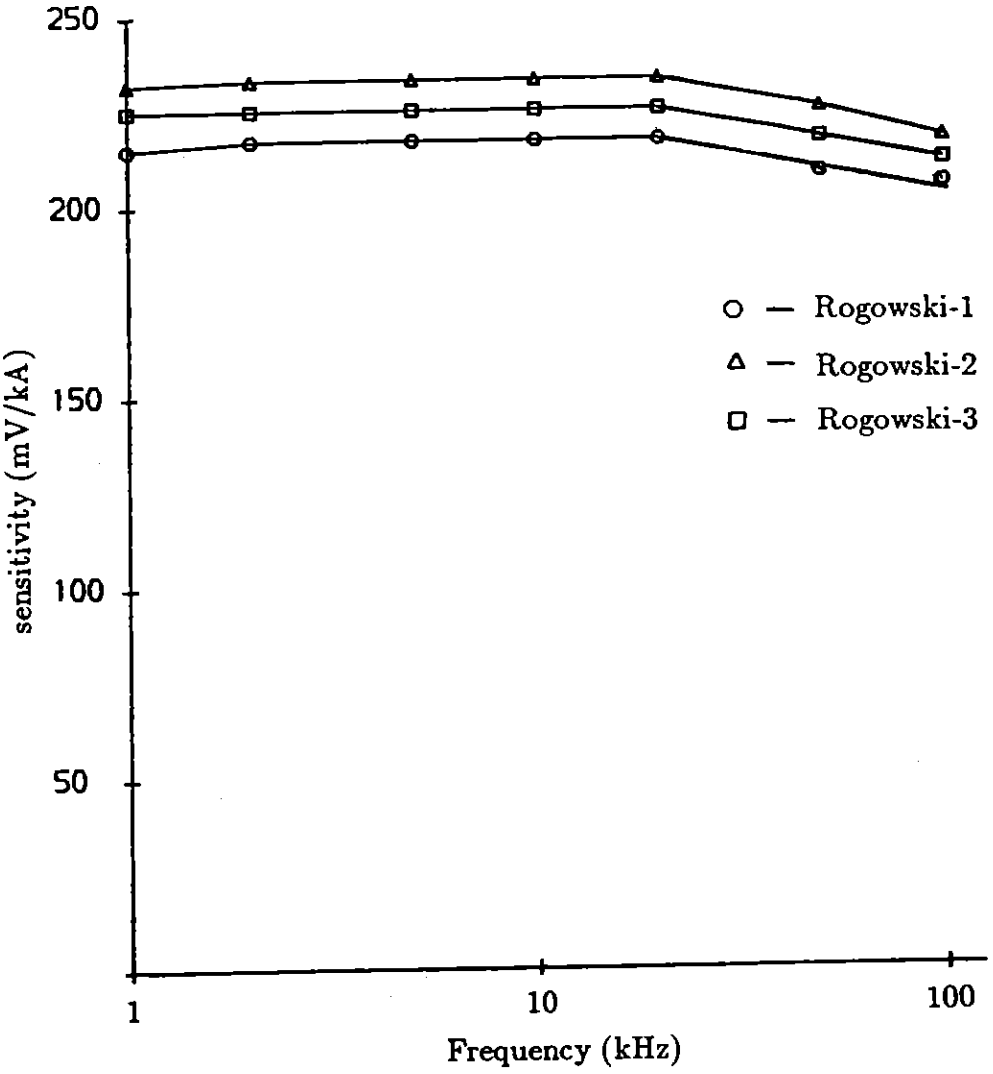

Figure 4.6 Frequency Response of the externally integrated Rogowski Coils used on the Rythmac devices.

Rogowski Coil	radius (mm)	number of turns	length (cm)	sensitivity (mV/kA)
Rythmac-1	7.5	370	40.3	217
Rythmac-2	7.4	417	45.6	233
Rythmac-3	7.2	583	63.4	225

Table 4.2: Rogowski Coil Specifications.
Note that sensitivity is at 20kHz.

Each Rogowski coil was calibrated together with its associated integrator, using a procedure similar to that used to calibrate the wire-wound probes. The Rogowski coils were calibrated by measuring the voltage output signal produced when a sinusoidal current of known amplitude and frequency was passed through their centres. The current was supplied by a Perreaux 8000B audio amplifier fed with a Datapulse Model 410 function generator. A calibrated Model 1025 Pearson current transformer was used to monitor the current. Figure 4.6 shows the frequency response of the externally integrated Rogowski coils obtained in the above manner. The coil sensitivities given in Table 4.2 were measured at a frequency of 20kHz. This choice of frequency is appropriate for a quasi-steady driven current pulse of $\sim 50\mu$s duration.

4.4 Loop Voltage Measurement

The loop voltage was measured in the Rythmac-1 device using a shielded single turn loop constructed from 50Ω triaxial cable as shown in Figure 4.7a. The loop, of radius $R_0 = 25$cm, was fastened to the top of the vacuum vessel and soldered together *in situ*. The loop voltage signal was attenuated and filtered with a 40kHz RC lowpass filter as shown in Figure 4.7b, before being displayed on an oscilloscope. The lowpass filter delays the loop voltage signal by approximately 6μs with respect to the Rogowski

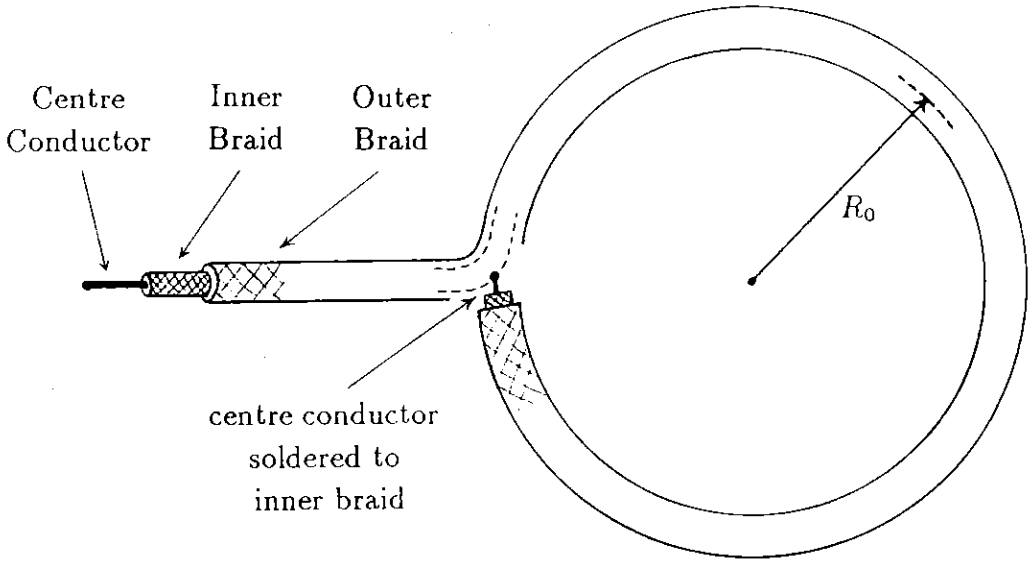

(a)

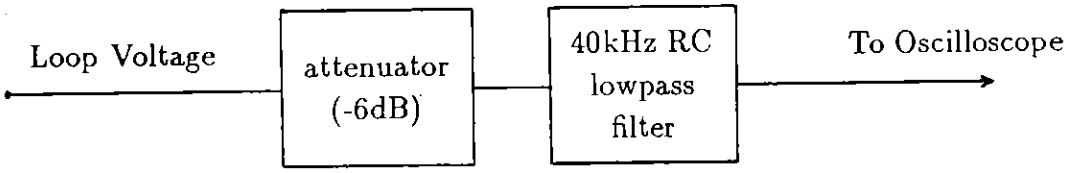

(b)

Figure 4.7 Loop Voltage measurements in Rythmac-1. (a) Schematic diagram of the coil which was constructed from 50Ω triaxial cable and used to measure the single turn Loop Voltage in Rythmac-1. (b) Signal processing for the coil output. Note that the lowpass filter introduces a delay of $\sim 6\mu$s into the loop voltage signal, which is evident in Figure 4.8

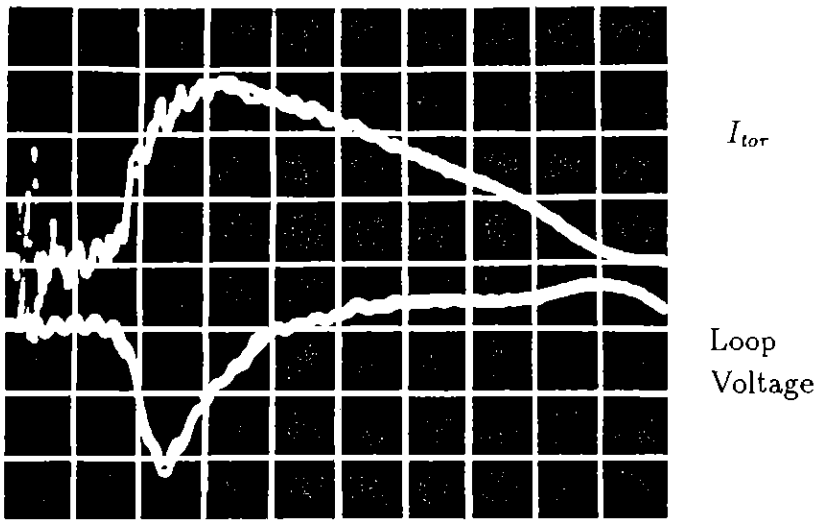

Figure 4.8 Oscillograms of the driven toroidal current and the single turn Loop Voltage measured in the Rythmac-1 device with the $m = 1$ double helix antenna. The signals from two plasma shots are overlaid to demonstrate the reproducibility of the discharges. Experimental conditions: filling pressure = 1.0mTorr of Argon, B_{tor} = 160G , B_v = 51G. The vertical scales are, I_{tor}: 461A/division and Loop Voltage: 10V/division (including the external 6dB attenuator). The timescale is 10μs/division.

belt measurement of the driven toroidal current.

In Figure 4.8, we show the driven toroidal current and the corresponding loop voltage signal for typical working conditions in the Rythmac-1 device. The signals from two plasma shots are overlaid to indicate the reproducibility of the data.

The loop voltage is a direct measurement of the back emf produced by the changing poloidal magnetic flux associated with the rapidly rising quasi-steady driven toroidal current. This back emf is capable of driving negative toroidal current along the path of minimum impedance. For a 'vacuum shot' with full RF current drive applied, the loop voltage is zero, unlike the loop voltage with a vacuum shot for an inductively driven tokamak.

In order to reduce the loop voltage and the possibility of inductively driven (negative) contributions to the total toroidal current, a short circuiting loop was installed at $r \simeq R_0$. The presence of the shorted turn was found to reduce the measured loop voltage by $\sim$ 50%, but did not significantly change the measured toroidal current waveform. The shorted turn was subsequently removed from the apparatus.

4.5 Data Acquisition System

The data acquisition system was based on a Digital Electronics Corporation (DEC) PDP-11/03 minicomputer and is shown schematically in Figure 4.9.

The incoming diagnostic signals were recorded and displayed on Tektronics 468 digital storage oscilloscopes which were interfaced to the PDP 11/03 via an IEEE General Purpose Interface Bus (GPIB). After each plasma discharge the digitised signals displayed on a 468 oscilloscope could be transferred via the IEEE Bus to the computer memory from where they were then written onto a flexible diskette. A total of three 468 oscilloscopes were connected to the IEEE Bus. The data acquisition software programs permitted the data obtained from each discharge to be uniquely labelled by the assignment of different extension numbers to the filenames. Differ-

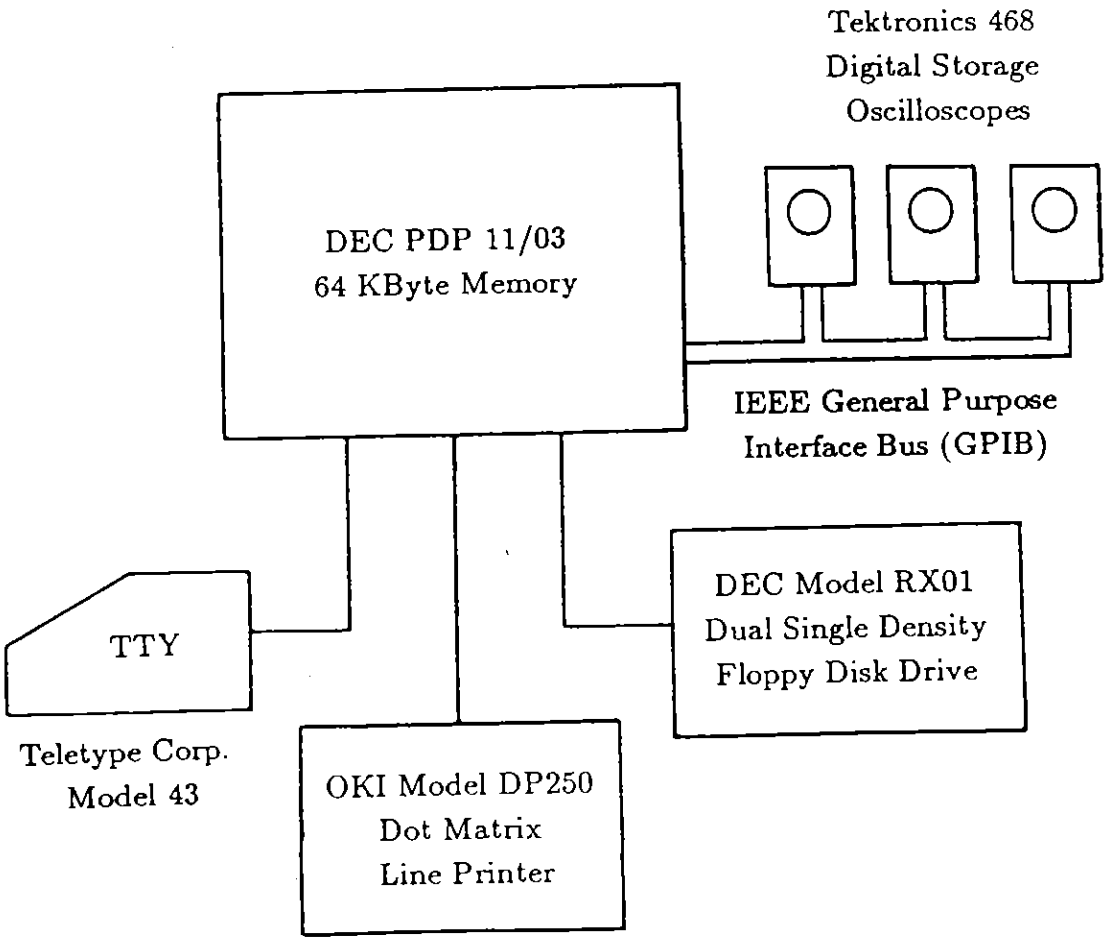

Figure 4.9 The digital data acquisition system.

ent filenames were used to identify the data received from each of the three digital oscilloscopes.

The data was analysed by either using the minicomputer system described here, or by electronically transferring the data via the computer network to the Flinders University physics research computer (Prime 750) which permitted more elaborate processing of large data files.